Influence of the water-skeleton interaction on the seismic response of earth dams

Youssef Parish[1,2], Isam Shahrour[1] and Marwan Sadek[1]
[1]Laboratoire de Mécanique de Lille (UMR – CNRS 8107)
Université de Lille 1 59650 Villeneuve d'Ascq, France
Isam.Shahrour@univ-lille1.fr
[2]The Institute for Energy and Hydro Technology (IEHT)
Tehran, IRAN

ABSTRACT
This paper presents a numerical analysis of the influence of the water-skeleton interaction on the response of earth dams to seismic loading. The non associated Mohr-Coulomb criterion is used for the description of the behaviour of earth material. Analysis is first conducted under undrained condition; then a full coupled analysis is used for the investigation of the influence of the water-skeleton interaction on the seismic response of the dam. Comparison of the undrained, full coupled and drained analyses shows that the undrained analysis overestimates the natural frequency of the dam and consequently could lead to a miss estimation of its response. The full coupled analysis predicts an important attenuation in the dam response, which could result from the role of the water flow in the dissipation of the seismic energy in addition to the influence of the induced pore-water pressure excess on the reduction of the effective stresses in the dam. As a consequence, full coupled analyses are recommended for the seismic design of earth dams.

Keywords: amplification, coupled, drained, earth dam, earthquake, plasticity, skeleton, undrained, water

1. INTRODUCTION

Dams and reservoirs located near urbanized areas represent a potential risk to the downstream population and property in the event of uncontrolled release of the reservoir water due to earthquake damage. The first failure of a dam due to earthquake reported in the literature is Augusta Dam, GA, during the 1886 Charleston, SC earthquake. Worldwide, about 30 dams have failed completely during earthquakes [1].

There are more than 75,000 dams of all sizes listed in the U.S. National Inventory of Dams [2] and thousands of large dams have been built worldwide. Hence, the record may appear outstanding. However, except for several well-known cases, few dams have been tested on ground motion equivalent to their Design Basis Earthquake [3]. Conversely, a few dams have experienced significant damage under moderate shaking. Performance data and detailed references regarding approximately 400 dams that have been subjected to significant earthquake shaking are provided by USCOLD [4, 5, 1].

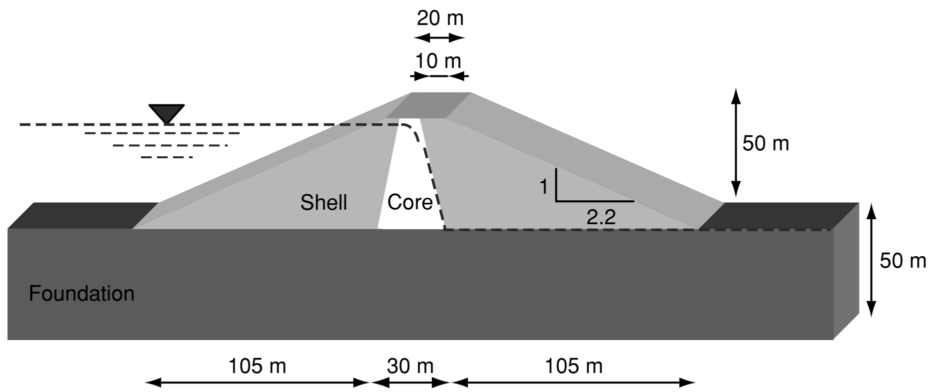

Figure 1 Problem under consideration: Influence of the water-skeleton interaction on the seismic response of an earth dam.

Seismic design of earth dams should take into consideration the influence of the water-skeleton interaction on the overall response of the dam. Since, the seismic loading is rapid with regard to the flow process in the core of the dam; engineers could use undrained analyses for dams design. This paper presents a confrontation of this approach to a full coupled approach that takes into account an effective stress formulation for the skeleton coupled to the Biot's formulation for the water-skeleton interaction [6, 7]. The paper does not deal with the liquefaction phenomena.

2. NUMERICAL MODEL

The problem under consideration is shown in figure 1. It concerns analysis of the influence of the water skeleton interaction on the response of an earth dam to seismic loading. A simplified configuration is considered in this analysis. The clay core is assumed to be homogeneous. An elastic perfectly plastic constitutive relation is used for the earth material. This model is based on the non associated Mohr-Coulomb criterion with tension cutoff. Although this model does not describe well the hardening of soils, it is largely used in geotechnical engineering; in addition the constitutive parameters of this model are usually available for different categories of soils. Rayleigh damping is used in the analyses with a damping ratio $\beta = 0.05$.

Numerical analyses are conducted using the FLAC program [8]. This program is based on a continuum finite difference discretization using the Langrangian approach. Every derivative in the set of governing equations is replaced directly by an algebraic expression written in terms of the field variables (e.g. stress or displacement) at discrete point in space [8]. For dynamic analysis, it uses an explicit finite difference scheme to solve the full equation of motion using lumped grid point masses derived from the real density surrounding zone. The calculation sequence first invokes the equations of motion to derive new velocities and displacements from stresses and forces. Then, strain rates are derived from velocities, and new stresses from strain rates. Every cycle around the loop correspond to one time step. Each box updates all of its grid variables from known values that remain fixed over the time step being executed.

Numerical distortion of the propagating wave can occur in dynamic analyses. Both the frequency content of the input motion and the wave-speed characteristics of the system will affect the numerical accuracy of wave transmission. Kuhlemeyer and Lysmer [9] showed that for an accurate representation of the wave transmission through the soil model, the spatial element size, Δl , must be smaller than approximately one-tenth to one-eighth of the wavelength associated with the highest frequency component of the input wave i.e.,

$$\Delta 1 \leq \lambda/10 \quad (1)$$

Where, λ is the wave length associated with the highest frequency component that contains appreciable energy. Expressing λ in the form of the shear wave velocity (V_S) and the highest frequency introduced to the system f_{max}, equation 1 can be written as:

$$\Delta 1 \leq V_S/(10\ .f_{\max}) \quad (2)$$

This requirement may necessitate a very fine spatial mesh and a corresponding small time step. The consequence is that reasonable analyses may be time and memory consuming. In such cases, it may be possible to adjust the input by recognizing that most of the power for the input history is contained in lower frequency components. By filtering the history and removing high frequency components, a coarser mesh may be used without significantly affecting the results.

The initial stress sate of the dam is determined using a static analysis of the dam response to gravitational forces.

In the full coupled analysis, the time step is determined in terms of the characteristic length of the mesh (L_c) and the diffusivity factor c as follows:

$$\Delta t = \frac{L_c^2}{c} \quad (3)$$

The diffusivity factor (c) is determined using the hydro mechanical properties of both the porous fluid and the porous media:

$$c = \frac{k}{\frac{1}{M} + \frac{\alpha^2}{K + 4G/3}} \quad (4)$$

K and G denote the bulk and shear modulus of the porous media, respectively. M, k and α stand for the Biot modulus, the mobility coefficient and the Biot coefficient, respectively.

3. INPUT MOTION

The seismic loading is applied at the base of the foundation layer as a velocity excitation. Analyses are conducted for two recorded earthquake motions. The first one corresponds to the Kocaeli earthquake in Turkey (1999) with a magnitude Mw = 7.4 [10]. The estimated peak velocity of this record is approximately equal to 0.40 m/sec (peak acceleration 0.247g), and its duration is approximately equal 30 sec (Figure 2a). The frequency of the major peak is equal to 0.9 Hz. The major part of the spectrum lies between 0.2 and 2Hz. The second input motion corresponds to Tabas earthquake in Iran (Figure 2b, [10]). The major peak corresponds to the frequency f = 0.5 Hz, the second peak appears at the

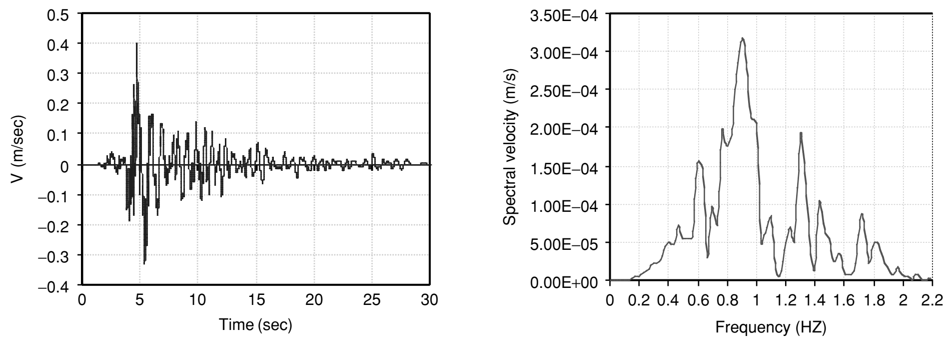

Figure 2a Kocaeli earthquake record (1999) a) Velocity, b) Spectrom.

frequency f = 1.1 Hz. The major part of the spectrum lies between 0.2 and 1.5 Hz. The duration is approximately equal 8 sec. Analyses were conducted with the magnitude of the Kocaeli record (V_a = 0.4 m/sec).

4. UNDRAINED ANALYSIS

The undrained analysis is conducted in total stresses. The shell material is assumed to be frictional, while that of the core is assumed to be purely cohesive. Geotechnical properties of the dam are summarized in table 1. The foundation material is assumed to be elastic with a Young's Modulus E = 1000 MPa. The Young's modulus of the core is equal to 40 MPa, while that of the shell is equal to 60 MPa. The Friction angle of the shell is equal to $\varphi = 35°$. The core cohesion (C_u) is assumed to increase with the initial effective vertical stress σ'_{v0} as follows:

$$C_u = \lambda_{cu}\sigma'_{v0} \tag{5}$$

Analyses were conducted with λ_{cu}=0.3

The response of the dam to the Kocaeli earthquake record is illustrated in figures 3 to 6. Figure 3 shows the distribution of plasticity in the dam at the peak of the excitation. It can be observed that plasticity is induced in the quasi totality of the dam. The residual displacement is presented in figure 4. It shows that the seismic loading induces a residual displacement in the upper part of the dam and at the extremities. The displacement attains 0.95 m. Figure 5 shows the displacement pattern in the axis and the middle height of the dam at the maximum excitation. It can be observed that the displacement in the axis of the dam increases first with the distance from the base up to a peak and then decreases. This variation corresponds to a combination of the first and second modes of the dam. The variation of the displacement at the middle height shows a sharp increase at the extremities; which could indicate the imminence of soil instability in this area.

Figure 6a shows the seismic amplification of the velocity in the dam. It can be observed that the amplification increases first with the distance from the base of the dam up to a peak and then decreases. This variation corresponds to a combination of the first two modes of the dam. Figure 6b shows the spectra of the velocity at the crest of the dam and the spectra of the input motion. It can be observed that the peak of the dam response occurs at the frequency f = 1.35 Hz ; a less pronounced peak appears at the frequency f = 0.64 Hz.

Figure 7a shows a comparison between the drained and undrained responses of the dam to Kocaeli earthquake record. It can be observed that the amplification of the tow responses

Table 1 Undrained analysis: properties of the earth dam

Parameter	Units	Core	Shell	Foundation
Dry density (*ρ*)	(kg/m^3)	1800	2000	2200
Saturated density (*ρ*')	(kg/m^3)	2100	2500	2500
Friction angle *(φ)*	(°)	0	35	
Cohesion *(c')*	(kPa)	$0.30*\sigma_{v0}'$	0.100	
Young's modulus *(E)*	(kPa)	40 000	60 000	1000 000
Poisson's ratio *(ν)*		0.3	0.3	0.25

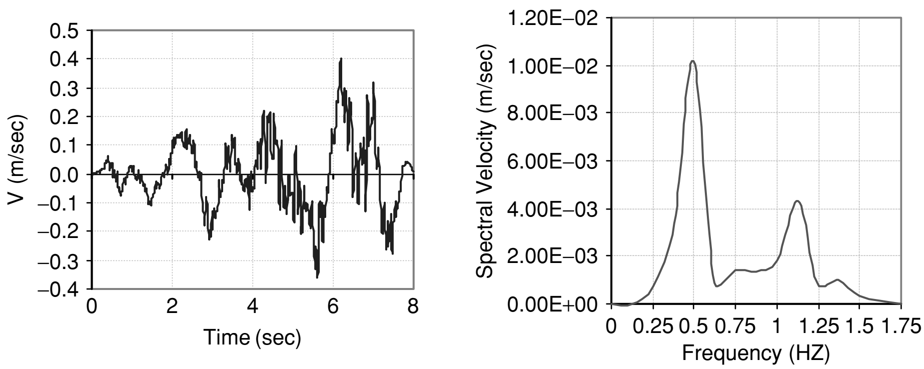

Figure 2b Tabas earthquake record: a) Velocity, b) Spectrom.

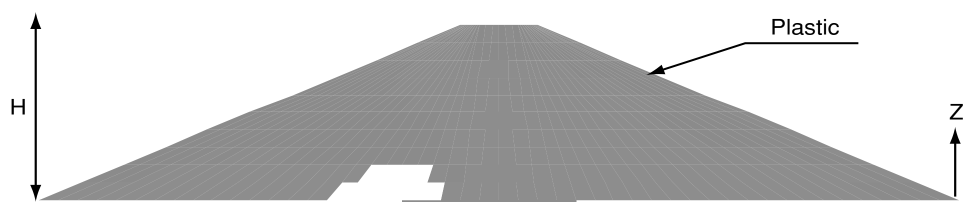

Figure 3 Undrained analysis: Distribution of plasticity in the dam (Maximum excitation) (Kocaeli earthquake record).

are close, except near the top of the dam, where drained response is higher than that the undrained one. Both of the responses correspond to a combination of the first and second modes, but the contribution of the second mode seems to be more important to the undrained response. Figure 7b shows the spectra of the drained and undrained responses of the dam. It confirms that the peaks of the drained and undrained responses occur at the frequency f = 1.35 Hz, which is close to the second frequency of the dam (f = 1.40 Hz).

Figure 8 shows a comparison of the seismic responses to Tabas and Kocaeli earthquake records. It can be observed that the amplification of the tow responses are very closes, except near the top of the dam, where the response to the Tabas input motion is higher than that to Kocaeli earthquake record (Figure 8a). The contribution of the second mode to the response to the Tabas input motion is less important than that to the response to Kocaeli reord. Figure 8b

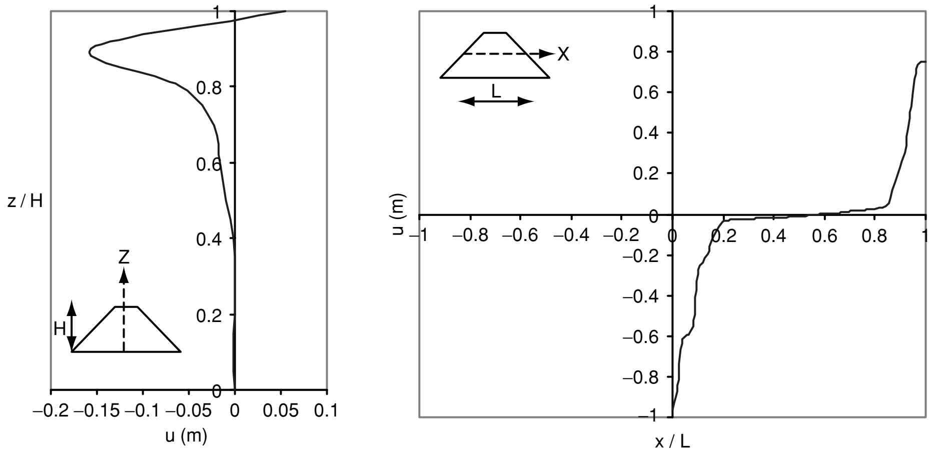

(Vertical axis of the dam) (Middle height of the dam)

Figure 4 Undrained analysis: Residual displacement in the dame axis and at middle height (Koaceli earthquake record).

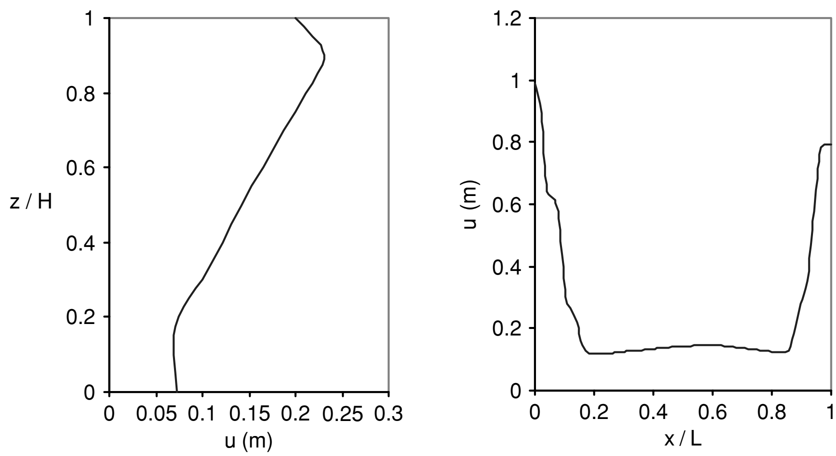

(Vertical axis of the dam) (Middle height of the dam)

Figure 5 Undrained analysis: displacement pattern at the maximum of the seismic excitation.

shows the spectra of the response to Kocaeli and Tabas earthquake records. It confirms that the peak of the response to Tabas record occurs at the frequency $f = 0.5$ Hz, which is lower than that of the response to Kocaeli earthquake record ($f = 1.32$ Hz).

5. FULL COUPLED ANALYSIS

Full coupled analysers are conducted using the effective stresses approach for the soil skeleton coupled to the Biot's formulation for the water-skeleton interaction.

The geotechnical properties of the dam are summarized in table 2. The foundation is assumed to be stiff with a Young's Modulus E = 1000 MPa. The Young's modulus of the core is equal to 40 MPa, while that of the shell is equal to 60 MPa. The friction angle of the shell

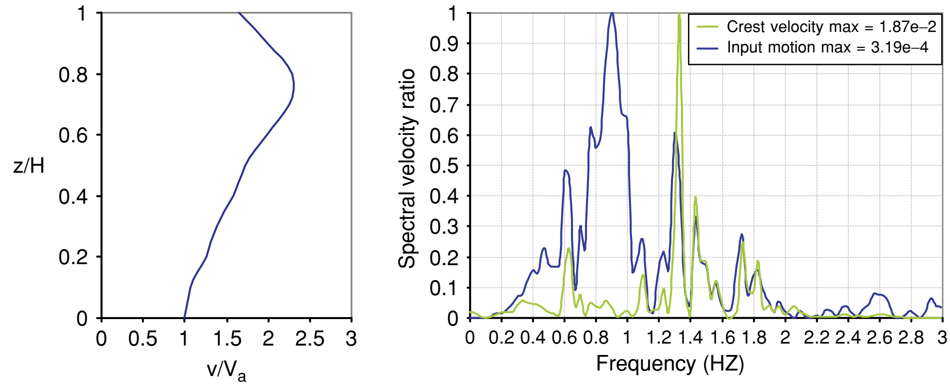

(a) Velocity amplification (b) Spectra of the dam response and the input motion

Figure 6 Undrained analysis: seismic amplification of the velocity . (Kocaeli earthquake record).

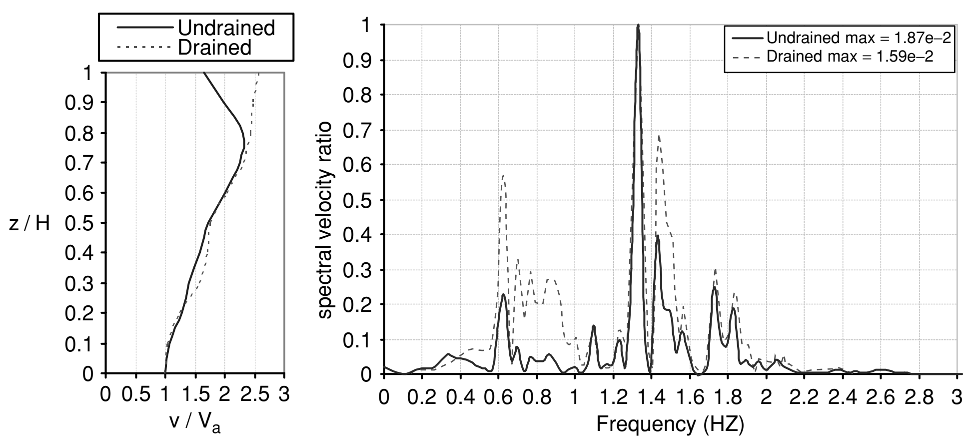

(a) Velocity amplification (b) Spectra of the dam response and the input motion

Figure 7 Comparison of the drained and undrained responses (Kocaeli earthquake record).

is equal to 35°. The cohesion and frictional angle of the core are equal to 100 kPa and 15°, respectively. The permeability of the core is equal to 9.810^{-7} m/s.

The dam response to Kocaeli earthquake input motion is illustrated in figures 9 to 13. Figure 9 shows the variation of the excess pore pressure ratio (R_u) at three positions of the dam: the base, the middle height and the top. This variation follows that of the input motion. At the top of the dam, (R_u) increases up to 1.16, while at the middle height it attains 1.1; at the bottom of the dam (R_u) decreases down to 0.9.

Figure 10 shows the displacement pattern in the axis and at the middle height of the dam at the maximum of the seismic excitation. It can be observed that the displacement in the axis of the dam increases with the distance from the base of the dam, with a quasi stabilization near the top of the dam. The variation of the displacement at the middle height shows a sharp increase at the extremities; which could indicate the imminence of a soil instability in this area.

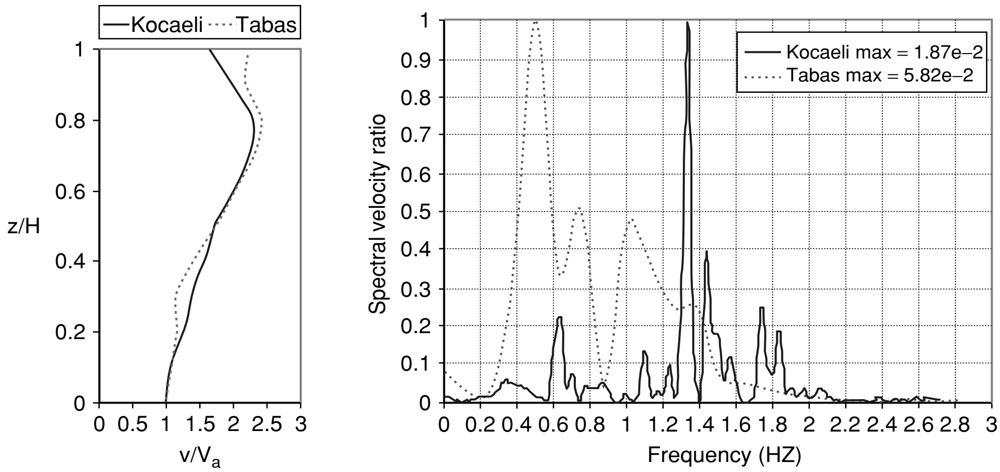

(a) Velocity amplification (b) Spectra of the dam response and the input motion

Figure 8 Comparison of the undrained responses to the Kocaeli and Tabas earthquake records.

Table 2 Full coupled analysis: properties of the earth dam

Parameter	Units	Core	Shell	Foundation
Dry density *(ρ)*	(kg/m^3)	1800	2000	2200
Saturated density *(ρ')*	(kg/m^3)	2100	2500	2500
Friction Angle *(φ)*	(°)	15	35	35
Dilation	(°)	3	10	3
Cohesion (*c'*)	(kPa)	0.1 e3	0.100	0.2e3
Young's modulus (*E*)	(kPa)	40000	60000	1000 000
Poisson's ratio (*ν*)		0.3	0.3	0.25
Elastic shear modulus *(G)*	(kPa)	15 000	23 000	400 000
Bulk modulus *(K)*	(kPa)	33 000	50 000	666 000
Porosity *(n)*		0.3	0.5	0.3
Permeability (k_h)	(m/ sec)	9.8e-7	9.8e-5	2.94e-4
Biot Modulus *(M)*	(kPa)	7.33e6	3.67e6	7.33e6
Mobility coefficient *(k)*	m^2/(sec*kPa)	5.00e-8	5.00e-6	1.35e-5
Diffusivity Factor *(c)*	m^2/sec	0.367	18.3	98.6

Figure 11 shows the amplification of the undrained and full coupled responses of the dam. It can be observed that the amplification of the undrained response is higher than that of the full coupled response. Both responses correspond to a combination of the first and second modes, but the contribution of the second mode seems to be more important to the undrained

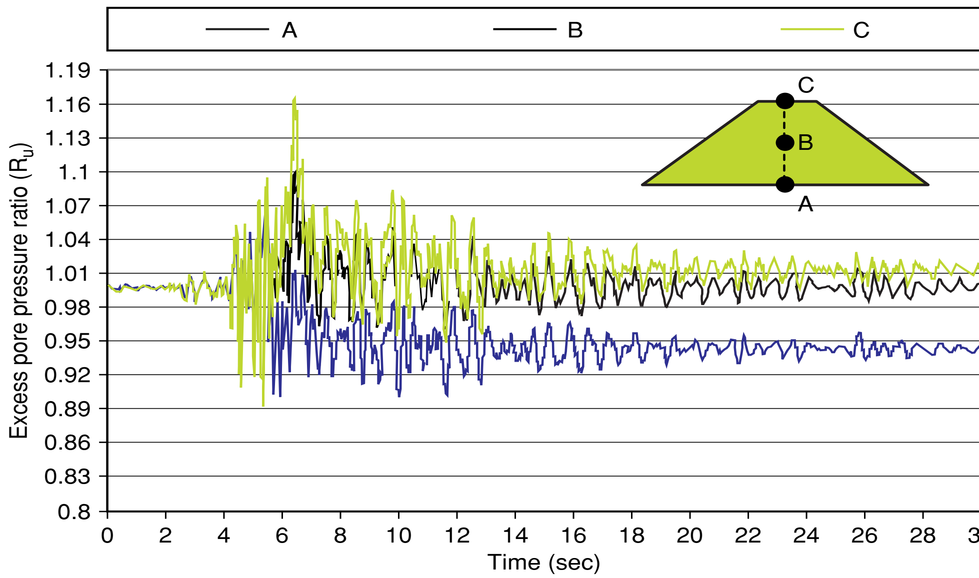

Figure 9 History of the excess pore pressure ratio at different points of the dam (Kocaeli earthquake record).

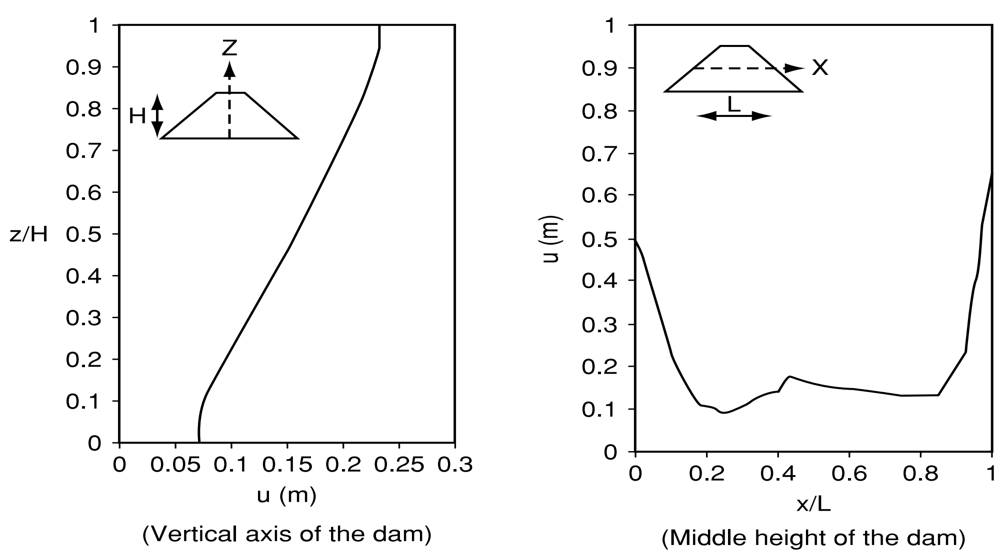

Figure 10 Full coupled analysis: Displacement at the maximum of seismic excitation (Kocaeli earthquake record).

response. Figure 12 confirms this observation. It shows that the full coupled response includes two peaks with equal values which correspond to the frequencies $f = 0.65$ Hz and 1.35 Hz, while the major peak of the undrained response occurs at the frequency $f = 1.35$ Hz. This result indicates that the undrained analysis could lead to an overestimation of the natural frequency of the dam, because of the overestimation of the dam stiffness.

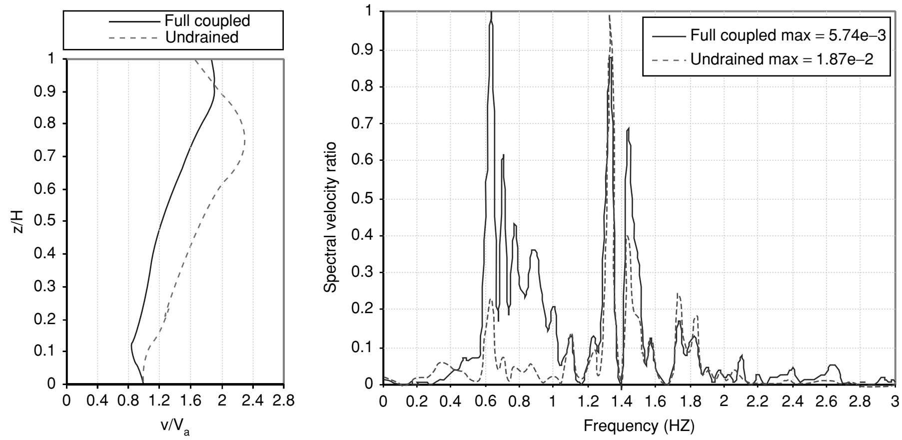

Figure 11 Comparison of the undrained and full coupled responses (Kocaeli earthquake record).

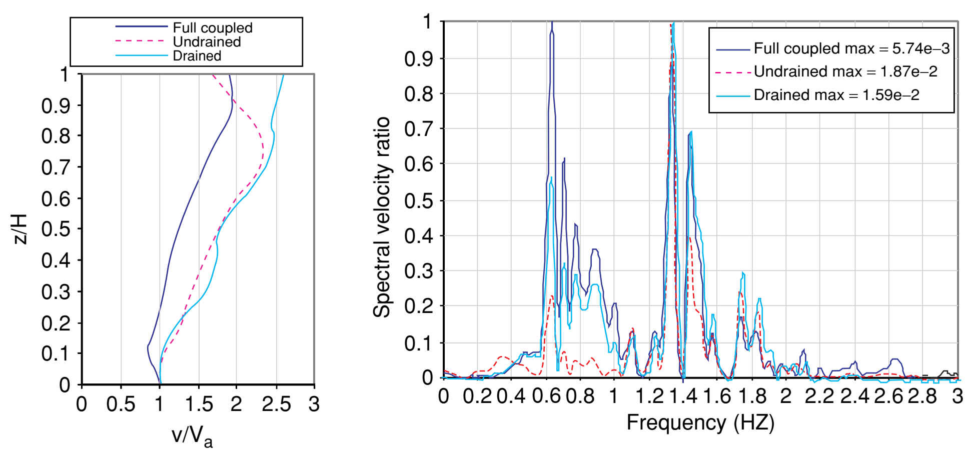

Figure 12 Influence of the water – skeleton interaction velocity amplification of the dam (Kocaeli earthquake record).

Figure 12 shows the influence of the water-skeleton interaction modelling on the response of the dam. It can be observed that the undrained analysis overestimates the natural frequency of the dam and could lead to a miss estimation of its response. The full coupled analysis shows an important attenuation of the dam response, which could result from the role of the water flow in the dissipation of the seismic energy in the dam in addition to the influence of the pore-water pressure increase on the reduction of the effective stresses and consequently to an increase in plasticity in the dam.

6. CONCLUSION

This paper included a study of the influence of the water-skeleton interaction on the seismic response of an earth dam. Investigations were conducted using undrained, full coupled and drained analyses for real earthquake input motions.

Results show that the undrained analysis overestimates the natural frequency of the dam and could lead to a miss estimation of its response. The full coupled analysis predicts an important attenuation in the dam response, which could result from the influence of the water flow in the dissipation of the seismic energy in addition to the influence of the induced pore-water pressure excess in the reduction of the effective stresses on the dam and consequently to an increase in the soil plasticity. These results show the necessity of the use of a full coupled analysis for the seismic design of earth dams.

REFERENCES

[1] USCOLD (U.S. Committee on Large Dams), 2000. "Observed Performance of Dams during Earthquakes," vol. II, Committee on Earthquakes, October, Denver, CO.

[2] U.S. Army Corps of Engineers. 1989.National Inventory of Dams (NID), April 2000 pdate, *U.S. Army Corps of Engineers, Washington, D.C.*

[3] USCOLD (U.S. Committee on Large Dams). 1999. "Updated Guidelines for Selecting Seismic Parameters for Dam Projects," *Committee on Earthquakes, April, Denver, CO.*

[4] USCOLD (U.S. Committee on Large Dams). 1984. "Bibliography on Performance of Dams during Earthquakes," *compiled by Philip Gregory, University of California, Berkeley*

[5] USCOLD (U.S. Committee on Large Dams), 1992b. "Observed Performance of Dams during Earthquakes," *Committee on Earthquakes, July, Denver, CO.*

[6] Zienkiewicz OC, Huang M, Pastor M. Numerical modeling of soil liquefaction and similar phenomena in earthquake engineering: state of the art. *Arulanandan K, Scott RF, editors. Verification of numerical procedures for the analysis of soil liquefaction problems*. Rotterdam: Balkema; 1994. p. 1401–14. ISBN 90 5410 360 4.

[7] Zienkiewicz OC, Leung KH, Hinton E, Chang CT. Liquefaction and permanent deformation under dynamic conditions—numerical solution and constitutive relations. *Pande GN, Zienkiewicz OC, editors. Soil mechanics, transient and cyclic loads. London: Wiley;* 1982. p. 71–103.

[8] Itasca Consulting Group, FLAC: Fast Lagrangian Analysis of Continua, *vol. I. User's Manual, vol. II. Verification Problems and Example Applications, Second Edition (FLAC3D Version 3.0)*, Minneapolis, Minnesota 55401 USA, 2005.

[9] R. L. Kuhlmeyer, and J. Lysmer, Finite Element Method Accuracy for Wave Propagation Problems, *J. Soil Mech. & Foundations Div., ASCE*, 99(SM5), 421–427, 1973.

[10] W.F. Chen, C. Scawthorn, *Earthquake Engineering Handbook, CRC Press LLC*, 2003.

[11] Regents of the University of California, PEER Strong Motion Database, *http://peer.berkeley.-edu/smcat/search.html*, P0141, Earthquake and Station Details, Tabas, Iran 1978/09/16, 2000.